3D PRINTING OF ANISOTROPIC METAMATERIALS

C. R. Garcia[1], J. Correa[1], D. Espalin[2], J. H. Barton[1], R. C. Rumpf[1, *], R. Wicker[2], and V. Gonzalez[3]

[1]EM Lab, W. M. Keck Center for 3D Innovation, University of Texas at El Paso, El Paso, Texas 79968, USA

[2]W. M. Keck Center for 3D Innovation, University of Texas at El Paso, El Paso, Texas 79968, USA

[3]Communications Laboratory, University of Texas at El Paso, El Paso, Texas 79968, USA

Abstract—Material properties in radio frequency and microwave regimes are limited due to the lack of molecular resonances at these frequencies. Metamaterials are an attractive means to realize a prescribed permittivity or permeability function, but these are often prohibitively lossy due to the use of inefficient metallic resonators. All-dielectric metamaterials offer excellent potential to overcome these losses, but they provide a much weaker interaction with an applied wave. Much design freedom can be realized from all-dielectric structures if their dispersion and anisotropy are cleverly engineered. This, however, leads to structures with very complex geometries that cannot be manufactured by conventional techniques. In this work, artificially anisotropic metamaterials are designed and then manufactured by 3D printing. The effective material properties are measured in the lab and agree well with model predictions.

1. INTRODUCTION

In the radio frequency (RF) and microwave regions, our ability to choose, or design, materials is quite limited due to the lack of molecular resonances at these frequencies. In contrast, a wide range of material options are available at optical frequencies because electron transitions are of this same time scale. Materials with striking color and strong dispersive effects are commonly available. At RF

and microwave frequencies, metamaterials are an attractive way to provide these same design options. Metamaterials are engineered composites that exhibit properties not found in nature and not observed in their constituent materials [1]. Many new and novel phenomena have been observed in metamaterials including negative refractive index [2–6], strong dispersion [7], anisotropy [8–11], and more. The most common form of metamaterials use subwavelength metal resonators to realize a permittivity [12] or permeability [13], but these structures are prohibitively lossy for many applications [14]. All-dielectric metamaterials can exhibit much lower loss than metal structures, but they offer fewer design options because they interact more weakly with an applied wave. Through clever engineering of their dispersion and anisotropy, many design options become possible including manipulation of polarization [15], stealth [16], mode transformers [17], wavefront reversal [18], and more. This approach, however, requires very complex geometries that cannot be manufactured by conventional technologies. 3D printing is ideally suited for this purpose because it is capable of placing different materials arbitrarily in three dimensions with high precision. To the authors' knowledge, this is the first demonstration of using 3D printing to manufacture all-dielectric anisotropic metamaterials.

This paper summarizes an artificially anisotropic metamaterial manufactured by 3D printing. First, the design methodology and optimization of a uniaxial metamaterial is discussed. Second, samples were manufactured using fused deposition modeling (FDM) and their dielectric tensor properties measured in the lab. The measured results agree well with the model predictions.

2. DEVICE DESIGN

The plane wave expansion method (PWEM) [19] was used to predict the effective tensor parameters of the anisotropic metamaterial. The method discretizes Maxwell's equations by expanding the field into a plane wave basis. This is highly efficient for all-dielectric structures with low to moderate dielectric contrast. Retrieving the constitutive parameters was simple because our structures operate in the long wavelength limit where branching [20, 21] does not occur. Given the dielectric function $\varepsilon\left(\vec{r}\right)$ of the unit cell and a Bloch wave vector $\vec{\beta}$, the PWEM solves Maxwell's equations as an eigen-value problem where the eigen-value is the square of the free space wave number k_0^2. To ensure the model operates in the long wavelength limit, the magnitude of the Bloch wave vector was made very small (i.e., $\beta < 0.5/a$). The effective refractive index of a Bloch wave can be calculated using

Eq. (1) by dividing the magnitude of the Bloch wave vector by the wave number of the first order band [21].

$$n_{eff} = \left|\vec{\beta}\right|/k_0 \tag{1}$$

In this work, an all-dielectric uniaxial metamaterial was designed. Being uniform in the z-direction, it was possible to model the device using a 2D PWEM code. In this case, Maxwell's equations decouple into two distinct modes, TM_z and TE_z. The TE_z mode has the electric field polarized in the x-y plane while the TM_z mode has the electric field polarized perpendicular to this plane. The ordinary refractive index n_o was retrieved by using a Bloch wave vector confined to the x-y plane. The direction within this plane was arbitrary due to the lattice having uniaxial symmetry. The extraordinary refractive index n_e was retrieved using a Bloch wave vector perpendicular to the x-y plane. Assuming there was no magnetic response in the bulk material, the dielectric tensor of the metamaterial along the principle axes was

$$\varepsilon_{r,eff} = \begin{bmatrix} n_o^2 & 0 & 0 \\ 0 & n_o^2 & 0 \\ 0 & 0 & n_e^2 \end{bmatrix} \tag{2}$$

A systematic study was performed to identify what types of easily fabricated structures exhibit the greatest anisotropy using a material with dielectric constant $\varepsilon_r = 2.57$. For the optimization, the strength of the anisotropy, or birefringence, was defined as the difference between the ordinary and extraordinary dielectric constants.

$$\Delta\varepsilon = n_e^2 - n_o^2 \tag{3}$$

The study included arrays of holes, arrays of dielectric rods, and different shaped holes and rods. Only square and hexagonal arrays were considered because only these are uniaxial in three dimensions. These combinations are illustrated in Figure 1. It was found that arrays of dielectric rods in air consistently produced stronger anisotropy than arrays of air holes in dielectric. Further, hexagonal arrays produced stronger anisotropy than square arrays due to the greater packing density of the rods. Of all the combinations, a hexagonal array of hexagonal shaped rods suspended in air provided the highest birefringence. Considering ease of design and manufacturing, a hexagonal array of circular rods was the final design. In addition, support features were added in order to produce a final lattice that is free standing and mechanically robust. To minimize their effect, supports were added along only two directions producing a lattice that was weakly biaxial, but still essentially uniaxial.

Given the basic design shown in Figure 2 a double parameter sweep was performed to determine the rod radius and thickness of the supports that maximize the birefringence. The dielectric was chosen to be polycarbonate (PC) which has a dielectric constant of $\varepsilon_r = 2.57$. The baseline unit cell and the data calculated from the double parameters sweep are provided in Figure 2. It was concluded from this data that the support features should be made as small as possible while still being mechanically robust. The radius of the dielectric rods that optimizes the anisotropy was found to be $0.42a$. Under these conditions, the dielectric tensor was calculated to be

$$\varepsilon_{\text{simulated}} = \begin{bmatrix} 1.8533 & 0 & 0 \\ 0 & 1.9535 & 0 \\ 0 & 0 & 2.0525 \end{bmatrix} \tag{4}$$
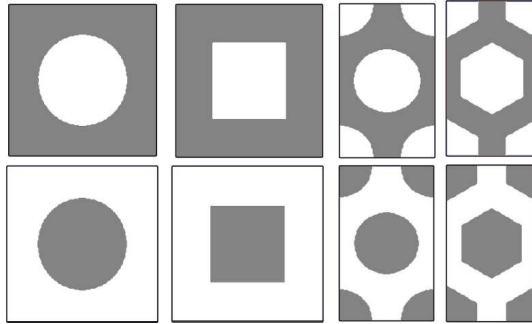

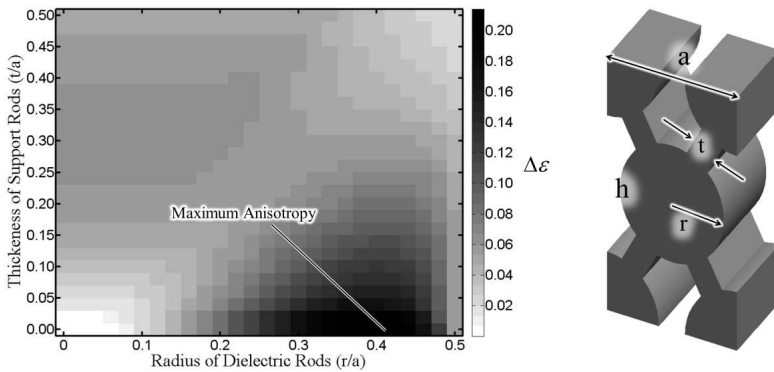**Figure 1.** Pictures of various unit cells simulated.

Figure 2. Double parameter sweep of anisotropic unit cell.

3. EXPERIMENTAL RESULTS

The final design dimensions were $a = 8.0$ mm, $r = 6.4$ mm, $h = 13.86$ mm, and $t = 1.8$ mm. The thickness of the rods t was determined by printing various test structures while shrinking the thickness each time until the mechanical integrity was no longer acceptable. The final device was manufactured by 3D printing using fused deposition modeling (FDM) [22]. First, a bulk sample of the PC material was printed and the dielectric constant was measured in the L-band (1.7–2.6 GHz) to be $\varepsilon_r = 2.57$ with a loss tangent of $\tan \delta = 0.02$. To measure the three tensor components of the metamaterial, three samples were printed in three orientations. The form factor was chosen to fit perfectly into a rectangular L-band waveguide with the dimensions of 109.22 mm × 54.61 mm × 35.56 mm. A photograph of these samples are shown in Figure 3.

Each sample was tested using the materials measurement software installed on an Agilent vector network analyzer (VNA). The transmission line method was selected for parameter retrieval [23] so the samples were inserted into a waveguide section and measured separately as shown in Figure 4. The dielectric constant of the x and y orientations should be equal because the metamaterial was uniaxial, but a small deviation in the symmetry was introduced during the manufacturing of about 1.25%. The final printed dimensions of the unit cell were $a = 8.1$ mm, $r = 6.5$ mm, $h = 13.8$ mm, and $t = 1.8$ mm.

The measured data over the L-band is provided in Figure 5. As anticipated, the x and y orientations were similar and the z orientation produced the largest effective dielectric constant. The measurements showed a sharp spike at the high frequency side of the spectrum. This is where the frequency is high enough that the resonant effects
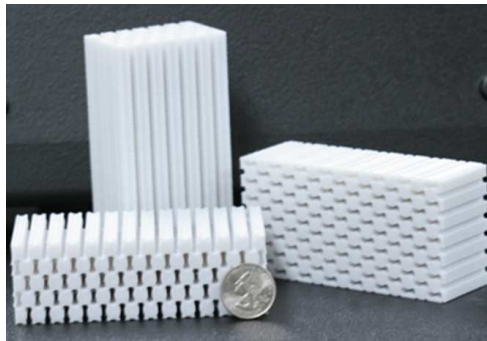

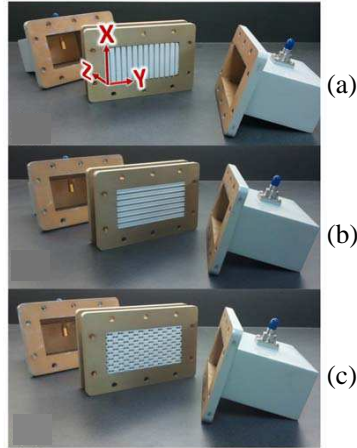**Figure 3.** Manufactured anisotropic metamaterials.

Figure 4. Materials under test. (a) Rods in the x-direction. (b) Rods in the y-direction. (c) Rods in the z-direction.
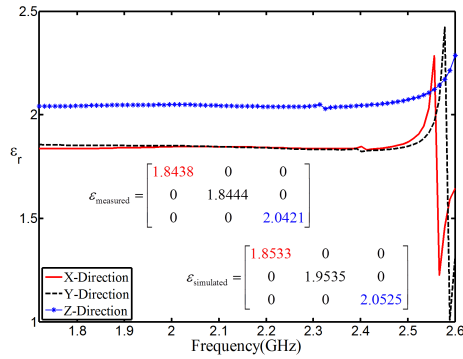

Figure 5. Measured dielectric tensor.

become significant. This represents the upper frequency cutoff of the metamaterial. It can be moved out to higher frequencies by reducing the lattice constant.

4. CONCLUSION

In this work, an all-dielectric uniaxial anisotropic metamaterial was successfully designed, fabricated, and tested. It was manufactured from polycarbonate using a form of 3D printing called fused deposition

modeling. The full dielectric tensor was measured in the lab and the experimental results corresponded well to the measured results. Future research in this area will include incorporating this basic design into microwave devices.

ACKNOWLEDGMENT

REFERENCES

1. Ramakrishna, S. A. and T. M. Grzegorczyk, *Negative Refractive Index Materials*, SPIE Press, Washington, 2009.
2. Kosaka, H., et al., "Superprism phenomena in photonic crystals," *Physical Review B*, Vol. 58, No. 16, R10096–R10099, 1998.
3. Pendry, J. B., "Negative refraction makes a perfect lens," *Physical Review Letters*, Vol. 85, No. 18, 3966–3969, 2000.
4. Shelby, R. A., D. R. Smith, and S. Schultz, "Experimental verification of a negative index of refraction," *Science*, Vol. 292, No. 5514, 77–79, 2001.
5. Smith, D. R. and N. Kroll, "Negative refractive index in left-handed materials," *Physical Review Letters*, Vol. 85, No. 14, 2933–2936, 2000.
6. Viktor, G. V., "The electrodynamics of substances with simultaneously negative values of ε and μ," *Soviet Physics Uspekhi*, Vol. 10, No. 4, 509, 1968.
7. Enoch, S., et al., "A metamaterial for directive emission," *Physical Review Letters*, Vol. 89, No. 21, 213902, 2002.
8. Genereux, F., et al., "Large birefringence in two-dimensional silicon photonic crystals," *Physical Review B*, Vol. 63, No. 16, 161101, 2001.
9. Grann, E. B., M. Moharam, and D. A. Pommet, "Artificial uniaxial and biaxial dielectrics with use of two-dimensional subwavelength binary gratings," *JOSA A*, Vol. 11, No. 10, 2695–2703, 1994.
10. Halevi, P., A. A. Krokhin, and J. Arriaga, "Photonic crystal optics

and homogenization of 2D periodic composites," *Physical Review Letters*, Vol. 82, No. 4, 719–722, 1999.

11. Smith, D. R., et al., "Design and measurement of anisotropic metamaterials that exhibit negative refraction," *IEICE Transactions on Electronics E Series C*, Vol. 87, No. 3, 359–370, 2004.

12. Rotman, W., "Plasma simulation by artificial dielectrics and parallel-plate media," *IRE Transactions on Antennas and Propagation*, Vol. 10, No. 1, 82–95, 1962.

13. Pendry, J., et al., "Magnetism from conductors and enhanced nonlinear phenomena," *IEEE Transactions on Microwave Theory and Techniques*, Vol. 47, No. 11, 2075–2084, 1999.

14. Soukoulis, C. M. and M. Wegener, "Optical metamaterials — more bulky and less lossy," *Science*, Vol. 330, No. 6011, 1633, 2010.

15. Hao, J., et al., "Manipulating electromagnetic wave polarizations by anisotropic metamaterials," *Physical Review Letters*, Vol. 99, No. 6, 63908, 2007.

16. Gaillot, D. P., C. Croënne, and D. Lippens, "An all-dielectric route for terahertz cloaking," *Opt. Express*, Vol. 16, No. 6, 3986–3992, 2008.

17. Mehta, A., et al., "Spatially polarizing autocloned elements," *Optics Letters*, Vol. 32, No. 13, 1935–1937, 2007.

18. Kukhtarev, N., "Wavefront reversal of optical beams in anisotropic media," *Quantum Electronics*, Vol. 11, No. 7, 878–883, 1981.

19. Leung, K. and Y. Liu, "Photon band structures: The plane-wave method," *Physical Review B*, Vol. 41, No. 14, 10188, 1990.

20. Datta, S., et al., "Effective dielectric constant of periodic composite structures," *Physical Review B*, Vol. 48, No. 20, 14936–14943, 1993.

21. Krokhin, A. A., P. Halevi, and J. Arriaga, "Long-wavelength limit (homogenization) for two-dimensional photonic crystals," *Physical Review B*, Vol. 65, No. 11, 115208, 2002.

22. Gibson, I., D. W. Rosen, and B. Stucker, *Additive Manufacturing Technologies, Rapid Prototyping to Direct Digital Manufacturing*, Springer, New York, NY, 2010.

23. Nicolson, A. M. and G. F. Ross, "Measurement of the intrinsic properties of materials by time-domain techniques," *IEEE Transactions on Instrumentation and Measurement*, Vol. 19, No. 4, 377–382, 1970.